

PAOS: a fast, modern, and reliable Python package for Physical Optics studies

Andrea Bocchieri¹, Lorenzo V. Mugnai², and Enzo Pascale¹

¹ Department of Physics, La Sapienza Università di Roma, Piazzale Aldo Moro 5, Roma, 00185, Italy ² School of Physics and Astronomy, Cardiff University, Queens Buildings, The Parade, Cardiff, CF24 3AA, UK

DOI: [10.xxxxxx/draft](https://doi.org/10.xxxxxx/draft)

Software

- [Review](#)
- [Repository](#)
- [Archive](#)

Editor: [Open Journals](#)

Reviewers:

- [@openjournals](#)

Submitted: 01 January 1970

Published: unpublished

License

Authors of papers retain copyright and release the work under a

Creative Commons Attribution 4.0 International License ([CC BY 4.0](#))

Summary

PAOS is an open-source code implementing physical optics propagation (POP) in Fresnel approximation and paraxial ray-tracing to analyze complex waveform propagation through both generic and off-axes optical systems. It enables the generation of realistic Point Spread Functions across various wavelengths and focal planes, and wavefront analyses at each point in the optical system. It improves upon other POP codes offering extensive customization options and the liberty to access, utilize, and adapt the software library to the user's application. With a generic input system and a built-in Graphical User Interface, PAOS ensures seamless user interaction and facilitates simulations. The versatility of PAOS enables its application to a wide array of optical systems, extending beyond its initial use case. PAOS presents a fast, modern, and reliable POP simulation tool, enhancing the assessment of optical performance for a wide range of scientific and engineering applications and making advanced simulations more accessible and user-friendly.

Developed using a Python 3 stack, PAOS is released under the BSD 3-Clause license and is available on [GitHub](#). The package can be installed from the source code or from [PyPI](#), so it can be installed as `pip install paos`. The documentation is available on [readthedocs](#), including a quick-start guide, documented examples, [jupyter](#) and [marimo](#) notebooks, a comprehensive description of the software functionalities, and guidelines for contribution. The documentation is continuously updated and is versioned to match the software releases.

PAOS was used in several scientific publications, including Mugnai et al. (2025), where it was used to generate the PSFs of the Ariel telescope, imported into the generic time-domain simulator of an exoplanet observation, [ExoSim 2](#). Bocchieri et al. (2025) then used ExoSim 2 with PAOS PSFs to develop an optimized algorithm for the jitter detrending of the Ariel observations. Besides ExoSim 2, PAOS is natively integrated into the generic point source radiometric simulator, [ExoRad 2](#) (Mugnai et al., 2023). In fact, these software packages are part of the same ecosystem, all developed to be generic and modular, adaptable to different applications, including but not limited to performance assessment of the Ariel mission. As an example, PAOS was used in Thurairethinam et al. (2025) as a POP tool to assess how wavelength-dependent phase errors caused by coating thickness non-uniformities in a dichroic degrade the optical performance. Finally, as a library, PAOS can be used to fit wavefront error maps to Zernike polynomials or orthonormal polynomials, and thus aid in the interpretation of interferometric measurements of surface errors and wavefront predictions from Structural Thermal Optical Performance (STOP) analyses, as implemented in the open-source code [STOP-utils](#).

Benchmark

We benchmarked PAOS against PROPER (Krist, 2007) on the HST optical system, because PROPER is not designed to handle a more complex optical system such as Ariel's, which i) is off-axis and ii) involves other elements than simple thin lenses (e.g. dichroics). The description of the HST system used is the one provided in the `Hubble_simple.py` file in the PROPER package¹. This description was translated into an input file² for PAOS. All simulation inputs have been matched (e.g., wavelength, grid size, zoom³). We added a line in the PROPER HST routine to set the pixel subsampling factor used to antialias the edges of shapes. We set this value to 101 from the default 11 to more closely match the exact treatment given in PAOS.

We compared the resulting PSFs at the focal plane of the telescope, both in the central region and in the outer wings. The first benchmark is reported below, showing the results for the PSFs at $1\ \mu\text{m}$. Figure 1 shows the central region of the HST PSFs as computed with PAOS and PROPER, and their difference. No significant residuals were found, with sporadic outlier pixels showing deviations by $< 0.1\ \text{dB}$ in regions corresponding to the PSF zeros due to small numerical errors.

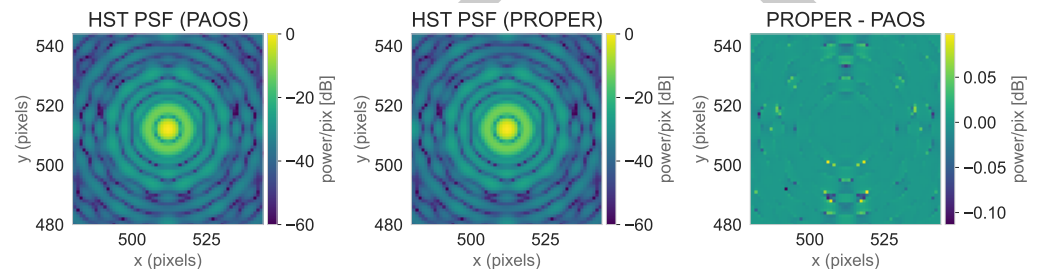


Figure 1: The central region of the HST PSF at $1\ \mu\text{m}$ as estimated with PAOS (left) and PROPER (center) and normalized to the maximum value in the array. The axes are in oversampled pixels. The color scale represents the power per pixel in decibels (dB), with a lower cut-off at -60 dB for better visualization. The right panel reports the difference between the PSF computed with PROPER and PAOS in the same physical units.

Figure 2 shows a detailed view of the slices of the PSFs along the horizontal and vertical axes, and their differences. The signal curves show an almost perfect overlap, with negligible residuals, all corresponding to values $< -50\ \text{dB}$ from the PSF maximum in the far wings.

¹The PROPER source code and documentation can be downloaded at <https://proper-library.sourceforge.net/>.

²`Hubble_simple.ini`, included in the package under the `lens` data directory for reproducibility.

³The ratio between the grid's linear dimension and the beam size at the initial surface.

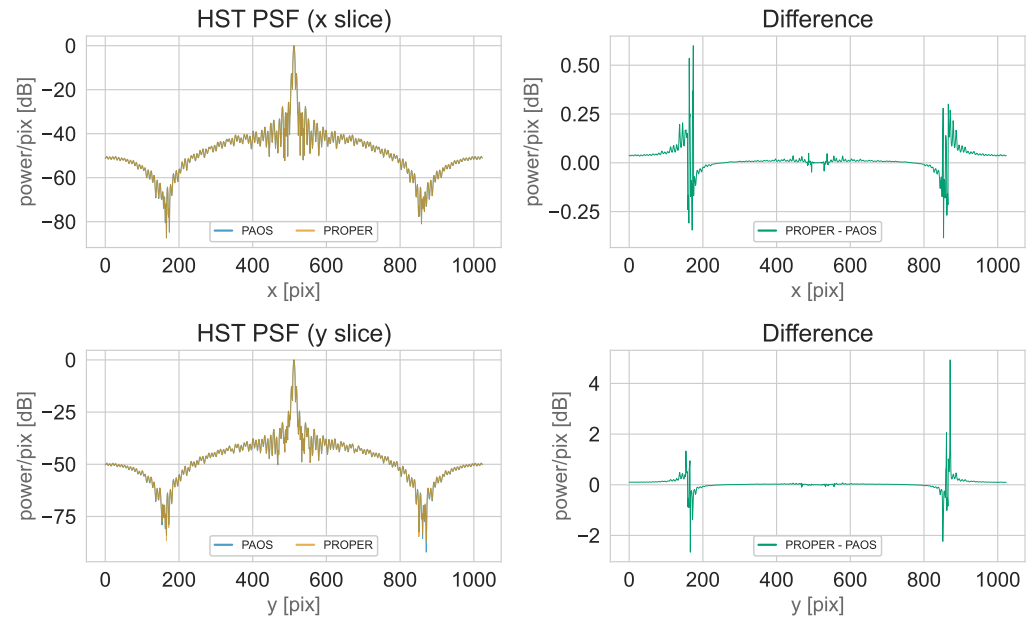


Figure 2: Comparison between PSF slices along the x and y axis, respectively. The left column reports the slice values for both codes, whilst the right column reports their difference. The units are the same (power per pixel in dB) to highlight even the smallest discrepancies. As can be observed, these differences are negligible for powers $\gtrsim -50$ dB for the HST application.

Figure 3 and 4 report the second benchmark; in this case, we simulate an aberrated HST PSF, where the wavefront error (WFE) is described by a superposition of Zernike polynomials. At M2, we added 100 nm RMS (WFE) each for defocus, vertical astigmatism, and oblique astigmatism, totaling $\sigma \approx 173.2$ nm WFE. The simulation is performed at $\lambda = 1.0 \mu\text{m}$; therefore, using the Ruze formula (Ross, 2009), the Strehl ratio is $S = \exp(-2\pi\sigma/\lambda) \approx 0.3$. Consequently, the PSF is highly aberrated and the main lobe is spread over more pixels. Thus, we can validate the PAOS implementation of optical aberrations, and we have a larger region of high signal. The latter is especially useful for investigating aliasing errors, which tend to occur more severely where the distribution has the highest amplitude because the amplitudes of the signal and the error add rather than the intensities (Lawrence et al., 1992).

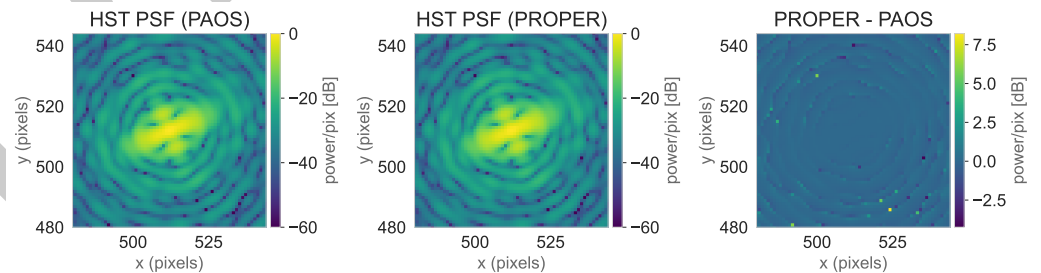


Figure 3: Same as Figure 1, but adding an optical aberration using Zernike polynomials: 100 nm RMS (WFE) for each of three low-order coefficients in the Zernike expansion: defocus and primary astigmatism (vertical and oblique), corresponding to the coefficients 4, 5, and 6 in the Noll ordering, respectively. The difference between the large-scale features of the PSFs is negligible.

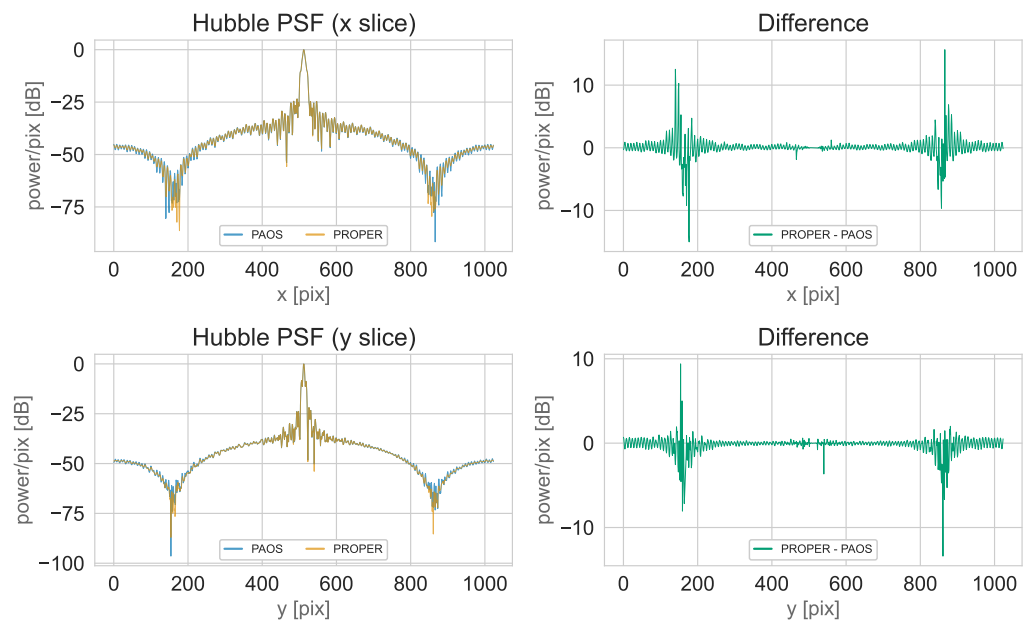


Figure 4: Comparison between the slices of the aberrated PSFs along the x and y axis, respectively. Locally, slightly hotter and colder pixels can be identified in the PSF wings, although, for powers $\gtrsim -50$ dB, this happens only sporadically. These minute numerical differences may be caused by the different treatment of aperture edges (exact for PAOS, sub-pixelled for PROPER), causing tiny aliasing errors.

We find that the differences between the aberrated PSFs are negligible and reach peaks of a few dB only in the far wings. However, even in the central region, there is an increase in hot and cold pixels compared to the unaberrated case. These discrepancies are probably due to the different treatment of the edges of apertures and vanes in the optical system, causing small aliasing errors when not exact. However, they are so tiny that they can be safely neglected for the HST application.

In summary, we find that PAOS is a robust and reliable tool for simulating the propagation of optical wavefronts through complex optical systems, as shown by the excellent agreement with the results obtained with PROPER for HST in our benchmark tests.

Statement of need

Accurate assessment of the optical performance of advanced telescopes and imaging systems is essential to achieve an optimal balance between optical quality, system complexity, costs, and risks. Optical system design has witnessed significant advancements in recent years, necessitating efficient and reliable tools to simulate and optimize complex systems (Smith, 2000). Ray-tracing and Physical Optics Propagation (POP) are the two primary methods for modelling the propagation of electromagnetic fields through optical systems. Ray-tracing is often employed during the design phase due to its speed, flexibility, and efficiency in determining basic properties such as optical magnification, aberrations, and vignetting. POP provides a comprehensive understanding of beam propagation by directly calculating changes in the electromagnetic wavefront (Goodman, 2005). POP is particularly useful for predicting diffraction effects and modelling the propagation of coherently interfering optical wavefronts. Yet, it may require supplementary input from direct measurements or a ray-tracing model for comprehensive analysis including aberration variations, especially in the Fresnel approximation. Commercial tools like Zemax and Code V enable POP calculations, offering advanced capabilities in aberration reduction and optical system optimization. However, these programs often come with substantial costs and steep learning curves, which may not be justifiable for every

95 application. Furthermore, accessibility to their source code is often limited or not available.

96 To address these limitations, we developed PAOS, a reliable, user-friendly, and open-source

97 POP code that integrates an implementation of Fourier optics. PAOS employs the Fresnel

98 approximation for efficient and accurate optical system simulations. By including a flexible

99 configuration file and paraxial ray-tracing, PAOS seamlessly facilitates the study of various

100 optical systems, including non-axial symmetric ones, as long as the Fresnel approximation

101 remains valid. Initially developed to evaluate the optical performance of the Ariel Space

102 Mission (Tinetti et al., 2018, 2021), PAOS has proven its value in assessing the impact of

103 diffraction, aberrations, and related systematics on Ariel's optical performance. By offering a

104 general-purpose tool capable of simulating the optical performance of diverse optical systems,

105 PAOS fills a crucial gap in the field and makes advanced physical optics research more accessible.

106 Acknowledgements

107 This work was supported by the Italian Space Agency (ASI) with Ariel grant n. 2021.5.HH.0.

108 References

- 109 Bocchieri, A., Mugnai, L. V., Pascale, E., & al., et. (2025). De-jittering Ariel: an optimized
- 110 algorithm. *arXiv e-Prints*, arXiv:2504.12907. <https://arxiv.org/abs/2504.12907>
- 111 Goodman, J. W. (2005). *Introduction to Fourier optics*.
- 112 Krist, J. E. (2007). *PROPER: an optical propagation library for IDL*. 6675, 66750P. <https://doi.org/10.1117/12.731179>
- 113 <https://doi.org/10.1117/12.731179>
- 114 Lawrence, G. N., Lawrence, & N., G. (1992). *Optical Modeling*. 11, 125. <https://ui.adsabs.harvard.edu/abs/1992aooe...11..125L/abstract>
- 115 <https://ui.adsabs.harvard.edu/abs/1992aooe...11..125L/abstract>
- 116 Mugnai, L. V., Bocchieri, A., & Pascale, E. (2023). ExoRad 2.0: The generic point source
- 117 radiometric model. *Journal of Open Source Software*, 8(89), 5348. <https://doi.org/10.21105/joss.05348>
- 118 <https://doi.org/10.21105/joss.05348>
- 119 Mugnai, L. V., Bocchieri, A., Pascale, E., Lorenzani, A., & Papageorgiou, A. (2025). ExoSim
- 120 2: the new Exoplanet Observation Simulator applied to the Ariel space mission. *arXiv e-Prints*, arXiv:2501.12809. <https://doi.org/10.48550/arXiv.2501.12809>
- 121 <https://doi.org/10.48550/arXiv.2501.12809>
- 122 Ross, T. S. (2009). Limitations and applicability of the maréchal approximation. *Appl. Opt.*,
- 123 48(10), 1812–1818. <https://doi.org/10.1364/AO.48.001812>
- 124 <https://doi.org/10.1364/AO.48.001812>
- 125 Smith, W. J. (2000). *Modern optical engineering: The design of optical systems*.
- 126 Thurairethinam, V., Bocchieri, A., Savini, G., Mugnai, L. V., & Pascale, E. (2025). Modeling
- 127 phase variations introduced by extreme broadband dichroics for astronomical photometry.
- 128 *Journal of Astronomical Telescopes, Instruments, and Systems*, 11(1), 014003. <https://doi.org/10.1117/1.JATIS.11.1.014003>
- 129 <https://doi.org/10.1117/1.JATIS.11.1.014003>
- 130 Tinetti, G., Drossart, P., Eccleston, P., & al., et. (2018). A chemical survey of exoplan-
- 131 ets with ARIEL. *Experimental Astronomy*, 46(1), 135–209. <https://doi.org/10.1007/s10686-018-9598-x>
- 132 <https://doi.org/10.1007/s10686-018-9598-x>
- 133 Tinetti, G., Eccleston, P., Haswell, C., & al., et. (2021). Ariel: Enabling planetary science across
- light-years. *arXiv e-Prints*, arXiv:2104.04824. <https://doi.org/10.48550/arXiv.2104.04824>
- <https://doi.org/10.48550/arXiv.2104.04824>